ISSN 1068-3666, Journal of Friction and Wear, 2014, Vol. 35, No. 1, pp. 32–39. © Allerton Press, Inc., 2014.
Original Russian Text © A.A. Fomin, A.B. Steinhauer, I.V. Rodionov, M.A. Fomina, A.M. Zakharevich, A.A. Skaptsov, A.N. Gribov, Ya.D. Karsakova, 2014, published in Trenie i Iznos, 2014, Vol. 35, No. 1, pp. 43–51.

Properties of Titanium Dioxide Coatings Produced by Induction-Thermal Oxidation of VT1-00 Alloy

A. A. Fomin[a, *], A. B. Steinhauer[a], I. V. Rodionov[a], M. A. Fomina[a], A. M. Zakharevich[b], A. A. Skaptsov[b], A. N. Gribov[b], and Ya. D. Karsakova[b]

[a]*Gagarin Saratov State Technical University, ul. Politekhnicheskaya 77, Saratov, 410054 Russia*
[b]*Chernyshevskii Saratov State University, ul. Astrakhanskaya 83, Saratov, 410012 Russia*
**e-mail: afominalex@rambler.ru*

Received April 10, 2013

Abstract—A new method of producing titanium dioxide coatings with a nanocrystalline structure on the surface of commercially pure titanium VT1-00 used in medicine is proposed. The morphological, physicomechanical, and tribological characteristics of the coatings formed by induction-thermal oxidation are studied. The obtained nanocrystalline and submicrocrystalline coatings have high hardness (4.23–9.86 GPa), modulus of elasticity (200–755 GPa), and scratching resistance (1.38–8.76 GPa); their coefficient of friction varies in a wide range (0.1–0.8).

Keywords: titanium dioxide, scratching resistance, hardness, induction-thermal oxidation, nanostructure, coating

DOI: 10.3103/S1068366614010036

INTRODUCTION

In modern dentistry, orthopedics, as well as anaplastic and oral surgery, supporting structures are generally made from biocompatible metals, mainly commercially pure titanium (VT1-00 and VT1-0) and its alloys (VT6 and VT16). These materials are used to produce elements of transosseous and intraosseous implants, as well as endoprostheses of large joints [1]. High characteristics of the biocompatibility of these metal implant structures are ensured by controlling the physicochemical, tribological, and biomechanical characteristics of their surface layers [2]. The metal base is responsible for the operation of an implant structure under the effect of multidirectional distributed loads; however, when an implant is installed into a prepared bone bed with a required interference, concentrated shear forces arise, which lead to a severe wear and a decrease in the biocompatibility of a surface layer [3]. As a result, under these extreme conditions, the strength characteristics of the surface, such as the hardness and the scratching resistance at the micro- and nanolevel, become of equal importance with the characteristics of biocompatibility [4, 5]. We would like to note that, provided that the structural integrity of these articles, including that of their surface layer in the form of a biocompatible functional coating, is retained, special attention is paid to the intensification of osteointegration processes by improving the morphology and geometrical characteristics, in particular the micron dimensions of elements of roughness and nanometer dimensions of elements of subroughness [6].

Coatings are usually produced on the surfaces of these structures using gas-thermal deposition; vacuum-condensation deposition (physical vapor deposition, PVD and chemical vapor deposition, CVD); oxidation, e.g., microarc, vapor-thermal, air-thermal, and argon–oxygen oxidation; and other less common methods [7]. The specific features of these technologies, which have become traditional, are high energy consumption and the cost of the raw materials, the complexity of the manufacturing sequence, and low output, as well as the low strength and wear resistance of the coatings, which have high porosity and a morphologically heterogeneous structure. As for achieving nanometer dimensions of structural elements, i.e., grains or pores, many of the above-mentioned methods have physical and technological limitations or utterly eliminate a possibility of forming these elements of the morphology of the surface layer; however, these elements are responsible for the improved biomechanical characteristics [6, 8].

Processes of the oxidation of refractory metals, including commercially pure titanium, were investigated by noted material scientists, such as P. Kofstad, D. I. Lainer, and R. F. Voitovich; more recent articles in this field have also been published [9]. Despite a large number of works that deal with modifying titanium and its alloys, the problem of producing interface coatings with high mechanical strength and scratching resistance, which should possess high char-

acteristics of biocompatibility when operating in an implant–bone medical bioengineering system, on surfaces of metal materials remains unsolved [8, 10].

The aim of this work was to determine the mechanical and tribological characteristics of biocompatible nanocrystalline and submicrocrystalline coatings with high mechanical strength and scratching resistance, as well as to develop recommendations on producing these coatings using a new efficient method of induction-thermal oxidation (ITO).

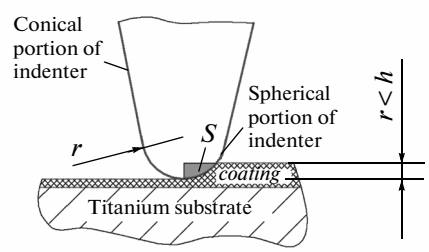

Fig. 1. Schematic of determining area of contact of indenter with coating during scratch tests.

EXPERIMENTAL

Biocompatible TiO_2 coatings were deposited on 2-mm-thick disk specimens made from commercially pure VT1-00 titanium. The preparation of the surfaces of the specimens included sand blasting by electrocorundum and ultrasonic cleaning. The prepared surfaces were intensively modified by oxidizing them in air using eddy currents generated by a high-frequency current (HFC) heating apparatus with a power of no more than 0.3 kW and a frequency of the current in the inductor of 100 ± 20 kHz [8]. The effect of ITO in a temperature range of 600–1200°C on the structural, physicomechanical, and tribological characteristics of the coatings, such as the hardness, the modulus of elasticity, the coefficient of friction, and the scratching resistance, was studied. The regimes of the treatment of the coating specimens were double numbered. The first number indicated the temperature of ITO (from 06 that corresponded to 600°C to 12 that corresponded to 1200°C), while the second number corresponded to the duration of ITO in seconds counted from the moment of the onset of the stationary oxidation regime. For example, the 08-030 regime corresponds to the temperature of ITO of 800°C and an ITO duration of 30 s.

The phase and structural states of the coatings were examined by X-ray diffraction (XRD) using a Gemini/Xcalibur diffractometer in CuK_α radiation ($\lambda = 1.541874$ Å), as well as by scanning electron microscopy (SEM) using a MIRA II LMU electron microscope equipped with an INCA PentaFETx3 detector for energy dispersive X-ray fluorescent analysis (EDX). The physicomechanical characteristics of the coatings were determined by nanoindentation, which made it possible to measure the hardness of thin coatings under a light load (10 mN) applied to a diamond Berkovich indenter, as well as by scratch tests, which revealed the mode of the fracture of the coatings scratched by a conical diamond indenter with a curvature radius of 10 μm under dynamic loads of 5–250 mN along a linear trajectory of up to 3 mm long. The scratch tests were carried out using a NANOVEA Ergonomic Workstation mechanical tester (ASTM E2546, ASTM C1624, ASTM G171, and ISO 20502). The scratch tests also made it possible to determine the coefficient of friction as a function of the depth of indentation and the corresponding normal load. These data were presented as a diagram that related the optical image of a scratch to the applied load, the depth of indentation, and the coefficient of friction. This allowed us to determine the scratch resistance of a coating over the fractured area and the mode of the fracture of the coating or its surface layer. The strength characteristic obtained is the ratio of the normal load P applied to the indenter to the area of contact S (Fig. 1). The area of contact is determined from the following expression for the half-area of the spherical segment:

$$S = \frac{2\pi rh}{2} = \pi rh = \left(31.4 \times 10^{-6}\right) h, \qquad (1)$$

where h is the height of the segment of the spherical portion of the indenter, m, and $r = 10$ μm is the curvature radius of the indenter.

RESULTS AND DISCUSSION

Under the considered conditions of ITO, the coatings of titanium dioxide TiO_2 are formed on the surface of titanium with an original α-Ti structure; in these coatings, titanium dioxide is present in the rutile phase. These changes in structural and phase states, which occur on the surfaces of the titanium specimens, are also confirmed by the XRD data (Fig. 2). In the thin oxide coatings, various types of defects are present, including through pores, which results in the appearance of peaks of the phase of the metal base in the spectra. The generalized XRD results for the specimens of the coatings are presented in Table 1.

In the surface layer of the titanium specimens, the following basic phases have been identified: the original α-Ti phase, which corresponds to the commercially pure titanium VT1-00; the basic phase of the TiO_2 oxide coating (rutile); and the secondary β-Ti phase, which results from moderate heat removal during cooling. This effect of the temperature occurs in the medium-temperature range of ITO (the regimes from series 08) near the α-Ti ↔ β-Ti solid-phase transformation and in the high-temperature range of ITO (the regimes from series 12) when the supply of the oxygen-containing medium is lacked. The free supply of the oxygen-containing medium favors the formation of a thick brittle oxide coating with a low

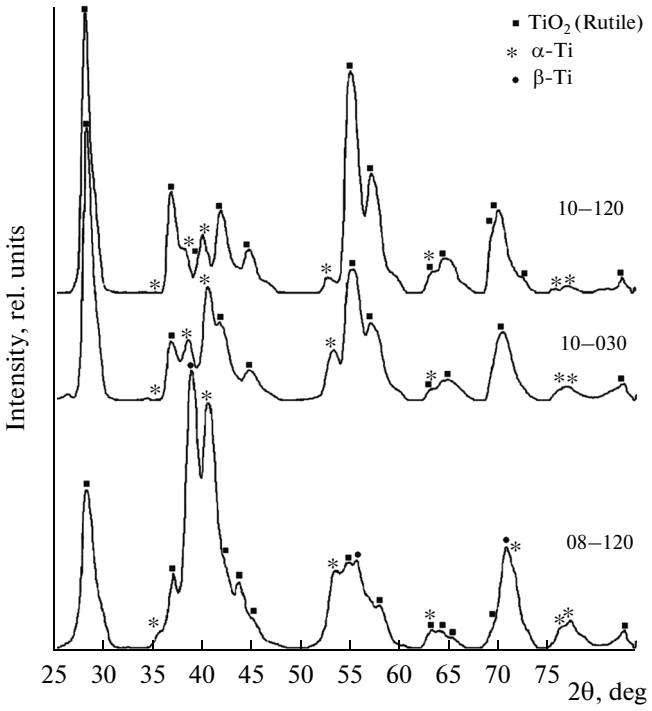

Fig. 2. Typical diffraction patterns of thin coatings produced using different ITO regimes: (bottom spectrum) 08-120, (middle spectrum) 10-030, and (upper spectrum) 10-120.

mechanical strength at the stage of intense HFC heating without exposure at a temperature of 1200°C (regime 12-001). When the specimens with the oxide coatings produced at these temperatures of ITO and duration of heating (30 s or longer) are cooled, these coatings spontaneously delaminate from the metal substrates. However, under conditions of the insufficient supply of oxygen (regime 12-001*), the thin sublayer formed on the surface of the titanium substrate has high physicomechanical and tribological characteristics, which will be considered below in more detail.

The morphology of the structure of the oxide coatings results from processes of intense oxidation, which occur during HFC heating. When describing the geometrical parameters of the crystalline structure, several types of the morphology were identified (Figs. 3 and 4). The shape of rutile crystals depends primarily on the ITO temperature; for example, at 800°C, the dimensions of longitudinal acicular nanocrystals increase to 70–100 nm (width) and 0.5–1.2 μm (length) (Fig. 3b). At a duration of ITO of over 150 s, the number of defects in the coating grows, which favors the formation of cleaved lamellar and prismatic crystals (Figs. 3c, 4b, 4c).

At a temperature of ITO of over 1000°C, the accelerated spontaneous delamination of a thick surface oxide layer occurs (Fig. 4a). In all likelihood, this is related to the process of the recrystallization of the titanium substrate and the growth of the internal submicron-sized layer, which is adjacent to the titanium substrate. The prismatic crystals result from the high-temperature effect of ITO under conditions of the insufficient supply of oxygen through the external thick layer of the oxides (Fig. 4c).

The titanium dioxide coatings have definite physicomechanical characteristics, including the hardness and the modulus of elasticity measured during nanoindentation (Table 2).

The dependence of the hardness of the TiO_2 on the temperature of ITO is parabolic. The minimum hardness corresponds to temperatures of 840–870°C, which can be explained by stresses that arise in the

Table 1. Phase composition of oxide coatings produced by ITO on commercially pure titanium VT1-00

Specimen	Regimes of ITO		Phase composition of coatings, %		
	temperature, °C	duration, s	α-Ti	β-Ti	TiO_2
06-300	600	300	47	0	53
08-030	800	30	100	0	0
08-120		120	36	41	23
08-300		300	44	35	21
10-001	1000	1	22	0	78
10-030		30	29	0	71
10-120		120	17	0	83
10-300		300	0	0	100
12-001	1200	1	29	0	71
12-001*		1	46	34	20
12-300*		300	28	55	17

* Specimens of coatings produced under conditions of insufficient supply of oxygen.

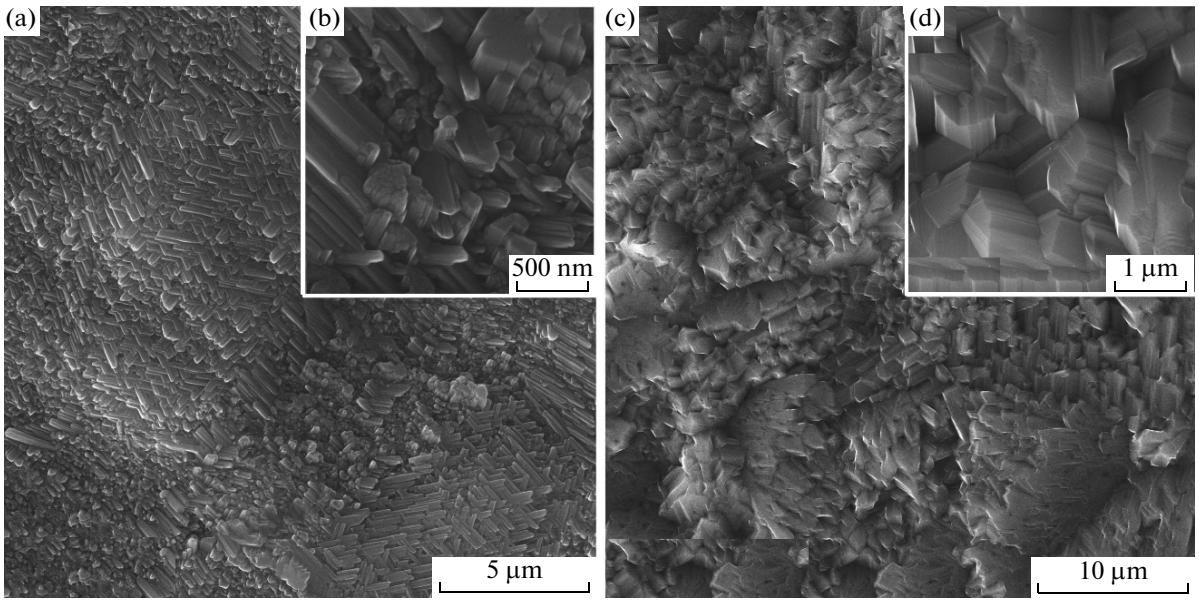

Fig. 3. Morphology of (a, c) microstructure and (b, d) nanostructure of TiO_2 coating produced using different ITO regimes: (left) 08-120 and (right) 10-120.

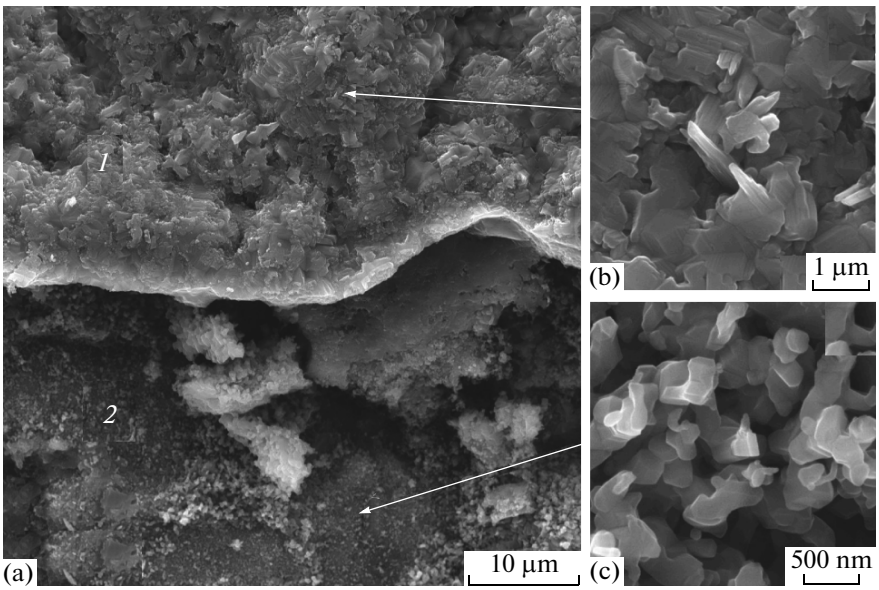

Fig. 4. (a) Morphology of laminated structure and (b, c) various types of crystals of TiO_2 coating produced using ITO regime 12-120: (*1*) thick outer oxide layer and (*2*) thin submicron inner layer adjacent to metal.

metal substrate and coating near the temperature of the $\alpha\text{-Ti} \leftrightarrow \beta\text{-Ti}$ phase transition. The above-described increase in the hardness in the high-temperature range occurs provided that the supply of air oxygen is lacking. Thus, the prismatic crystals have both the developed morphology of the surface and the high mechanical strength characteristics (Fig. 4). The obtained values of the mechanical characteristics are indicative of the high strength of these coatings, which is confirmed by the 2–3.5-fold reserve of the hardness in comparison with the titanium substrate and the 8–15-fold reserve of the hardness compared with the cortical bone tissue.

The obtained data on the hardness of the coatings correlate with their high scratch resistance, which is well illustrated by the results of optical-microscopic examination and the scratch-test diagrams (Figs. 5a and 5b). In the diagram for specimen 10-001, the test parameters are presented, including the axial load, which is applied to the indenter and gradually varies by

Table 2. Mechanical characteristics of biocompatible titanium dioxide coatings

Specimen	Hardness, GPa	Modulus of elasticity, GPa
Cortical bone	0.64 ± 0.05	6.12 ± 0.74
Titanium VT1-00	2.27 ± 0.41	119.0 ± 3.9
06-120	5.28 ± 0.71	237.0 ± 22.5
08-120	4.23 ± 0.44	201.3 ± 16.5
10-120	6.93 ± 0.51	337.6 ± 33.3
12-120*	9.86 ± 0.54	754.6 ± 69.0

* Specimens of coatings produced under conditions of insufficient supply of oxygen.

the linear law (Fig. 5b). Based on the simple geometrical concepts of the shape of the surfaces in contact and using expression (1), we calculate mechanical stresses that arise during fracture. According to the microscopic examination data for the scratch and taking into account the coefficient of friction that, between a normal load of 220 mN and a depth of indentation of 1.5 μm and a load of 225 mN and a depth of indentation of 4.4 μm, has increased from 0.6 to 0.9, we obtain the following strength characteristics: the ultimate strength in the scratch test is about 4700 MPa and the residual resistance after the fracture of the coating is about 1600 MPa. Thus, the results of the scratch tests of the coatings under study have shown their high scratching resistance. The scratch-test data and their relation to a type of the structure of the coatings and their surface layers are generalized in Tables 3 and 4.

The use of the SEM in combination with the EDX of the chemical composition of different portions of the specimens under study has allowed us to investigate in more detail the mode of fracture during scratching and the corresponding structural transformations in the surface layer of titanium. The portions of the scratch that correspond to the initial stage of the fracture of the coating or the end of the test upon achieving the maximum load were examined (Fig. 6).

The presented examples of the images of the portions of the scratches show the typical modes of fracture. The thin coating is entirely worn out up to the metal substrate (Fig. 6a). This is completely confirmed by the results of EDX, which show that, in the middle part of the cross sections of the scratches, the concentration of oxygen substantially decreases (up to 0%) (Table 5). In the case of the thickened or thick coating with high hardness and scratching resistance deposited to the soft metal substrate, the penetration of the coating material to the substrate is observed (Figs. 6c, 6d). During scratching, high tangential stresses arise in the coating material, which result in the delamination of

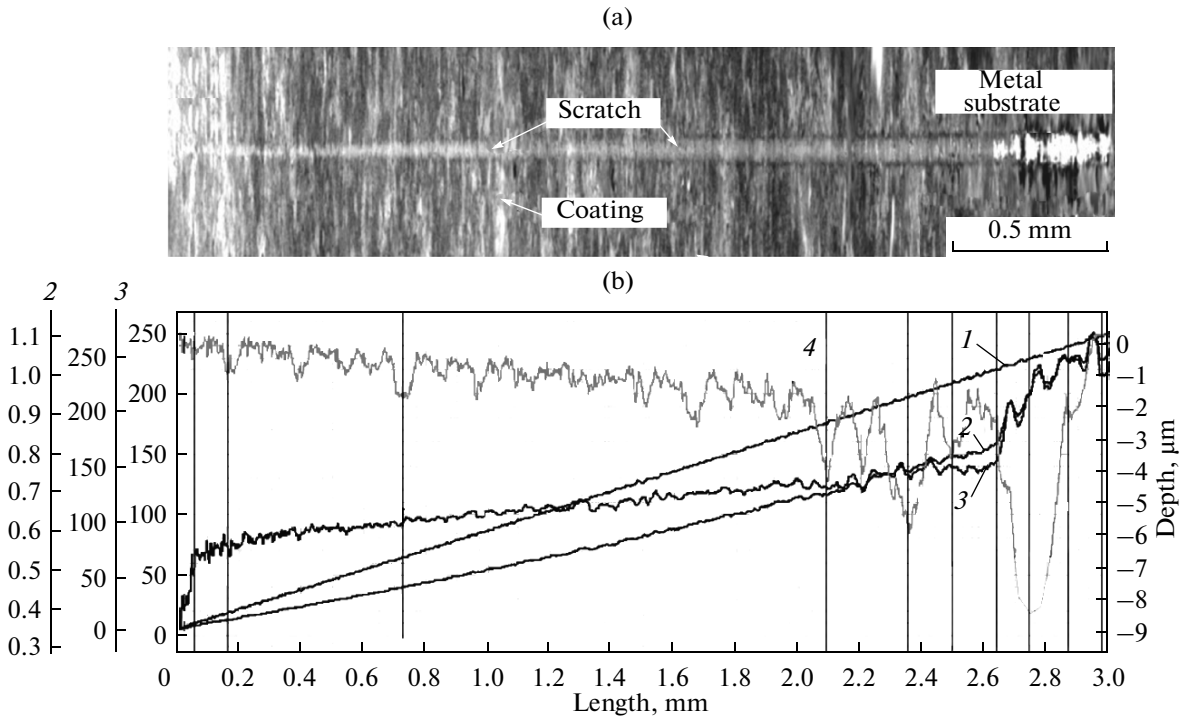

Fig. 5. Result of scratch test of specimen produced using ITO regime 10-001: (a) morphology of surface and (b) diagram of variations in characteristics under consideration; (*1*) basic load, mN; (*2*) force of friction, mN; (*3*) coefficient of friction; and (*4*) depth of penetration, μm.

Table 3. Generalized scratch-test data for titanium dioxide coatings produced by ITO on titanium VT1-00

Specimen	Parameters of scratch tests carried out directly (1) before and (2) immediately after moment of fracture of coating or surface layer					
	axial load P_1, mN	depth of indentation h_1, μm	range of coefficient of friction k_1*	axial load P_2, mN	depth of indentation h_2, μm	range of coefficient of friction k_2*
Titanium VT1-00	50	7.0	0.1 → 0.5	–	–	0.5 → 0.9
06-300	90	1.5	0.1 → 0.3	100	2.0	0.7 → 0.95
08-030	130	1.4	0.1 → 0.3	150	3.7	0.4 → 0.95
08-120	190	1.6	0.05 → 0.23	195	3.1	0.27 → 0.41
08-300	110	1.5	0.11 → 0.19	120	3.0	0.29 → 0.34
10-001	220	1.5	0.52 → 0.80	225	4.4	0.92 → 1.10
10-030	150	1.4	0.11 → 0.20	165	2.4	0.26 → 0.30
10-120	68	0.5	0.05 → 0.16	70	1.0	0.17 → 0.33
10-120**	165	0.6	0.45 → 0.75	175	5.2	0.75 → 0.94
10-300	160	1.0	0.10 → 0.17	170	3.3	0.20 → 0.25 → 0.30
12-001	100	1.0	0.09 → 0.20	–	–	–
12-001**	205	2.0	0.14 → 0.18	210	6.0	0.45–0.78 → 0.36
12-300	130	3.0	0.15 → 0.25	150	12.0	0.13 → 0.23

* Changes in coefficient of friction are indicated by the sign from the beginning to the end of ranges 1 and 2.

** Data for interlayer.

Table 4. Structural organization of coatings and surface layer of specimens

Specimen	Description of structure
Titanium VT1-00	Metal surface of prepared titanium (α-Ti) plates after machining (fine grinding), which is characterized by low degree of strain hardening
06-300	Thin nanocrystalline coating + α-Ti surface layer
08-030	Thin homogeneous nanocrystalline coating + α-Ti surface layer
08-120	Thin homogeneous nanocrystalline coating + (α-Ti + β-Ti) surface layer
08-300	Thin homogeneous submicrocrystalline coating + (α-Ti + β-Ti) surface layer with increased concentration of oxygen
10-001	Thin homogeneous nanocrystalline coating + α-Ti surface layer
10-030	Thin submicrocrystalline coating + α-Ti surface layer
10-120	Thick submicrocrystalline outer coating
10-120*	Submicrocrystalline underlayer of coating + α-Ti soft surface layer
10-300	Thick submicrocrystalline outer coating + submicrocrystalline underlayer of coating (no spontaneous delamination have been observed)
12-001	Thick submicrocrystalline outer coating (delamination due to mechanical effect)
12-001*	Submicrocrystalline underlayer of coating + (α-Ti + β-Ti) surface layer
12-300	Sintered highly-porous thick submicrocrystalline outer coating (no spontaneous delamination have been observed)

particles from the coating (Fig. 6b). The migration of the aluminum impurity present in the VT1-00 alloy toward the surface of the coating occurs, and alumina can be formed.

Thus, the results of the scratch tests, as well as the data on the permissible load P_1 and the depth of indentation h_1, which does not lead to the fracture of the functional coating, have allowed us to determine the

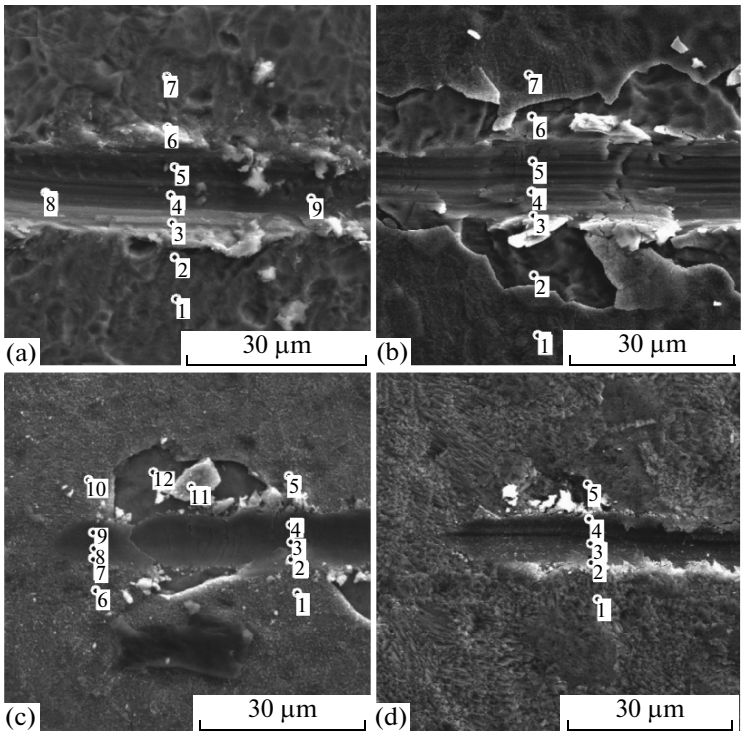

Fig. 6. SEM images of scratches on specimens of coatings produced using different ITO regimes: (a) 06-300; (b) 08-030; (c) 08-300; and (d) 10-030. Magnification ×3000.

quantitative strength characteristic of the scratching resistance (Fig. 7). Using the values of the load P_2 and the depth of indentation h_2, the residual strength can be estimated for the coating after stress relaxation and the formation of a cracked structure. The approximation of the experimental data on the ultimate strength in scratching σ_{SR} as a function of the temperature T and the duration t of ITO is described fairly well by the following third-degree polynomial:

$$\sigma_{SR} = 83\,598 - 312.14T - 45.16t + 0.38T^2 + 0.81t^2 - 1.49T^3 - 2.20t^3. \quad (2)$$

Table 5. Differential distribution of chemical elements in coating and surface layer

Number of spectrum	Specimen											
	06-300			08-030			08-300			10-030		
	O	Al	Ti	O	Al	Ti	O	Al	Ti	O	Al	Ti
1	38.67	0.32	61.02	57.29	0.39	42.32	66.94	0.36	32.70	62.76	0.58	36.66
2	31.41	0.00	68.59	25.09	0.41	74.50	74.07	0.24	25.69	73.21	0.00	26.79
3	0.00	0.91	99.09	17.01	0.43	82.56	65.99	0.00	34.01	67.53	1.03	31.44
4	0.00	1.58	98.42	0.00	0.00	100.0	56.21	0.00	43.79	60.70	0.32	38.97
5	0.00	0.77	99.23	0.00	0.53	99.47	63.74	0.43	35.84	43.76	0.00	56.24
6	56.69	0.51	42.80	22.02	0.41	77.57	63.84	0.38	35.77	–	–	–
7	40.10	0.35	59.55	48.54	0.51	50.96	70.93	0.29	28.78	–	–	–
8	0.00	0.81	99.19	–	–	–	68.37	0.31	31.31	–	–	–
9	0.00	1.18	98.82	–	–	–	54.29	0.41	45.30	–	–	–
10	–	–	–	–	–	–	52.57	0.43	47.01	–	–	–
11	–	–	–	–	–	–	65.24	0.49	34.28	–	–	–
12	–	–	–	–	–	–	43.93	0.36	55.71	–	–	–

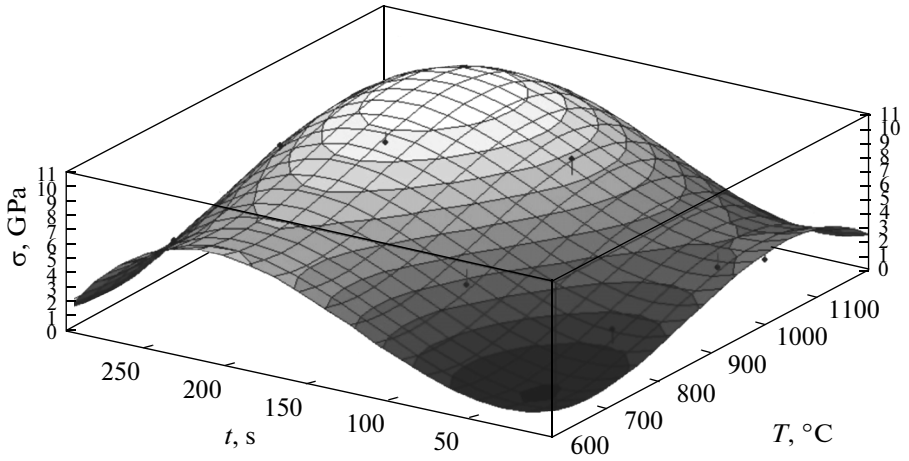

Fig. 7. Dependence of ultimate strength of coating in scratching on parameters of ITO.

CONCLUSIONS

After ITO, the structure of the surface of the commercially pure titanium VT1-00 is characterized by the formation of the titanium dioxide coating with high characteristics of morphological heterogeneity, as well as high physicomechanical and tribological characteristics. The titanium dioxide coatings are made up of nano- and submicron-sized acicular, lamellar, and prismatic crystals. The effect of the parameters of the ITO process on the chemical composition and the phase and structural parameters, as well as the mechanical and tribological characteristics of the coatings, has been established. Using ITO regimes 06-120, 08-120, 10-001, and 12-001, the coatings with the best characteristics of morphology, as well as an increased hardness (4.23–9.86 GPa) and a scratching resistance of no less than 3.78–8.76 GPa, were produced; when the 10-120 regime with an insufficient supply of oxygen was used, the characteristics of the coatings were highest.

ACKNOWLEDGMENTS

This study was supported in part by the Russian Foundation for Basic Research (project no. 13-03-00898 a), the Ministry of Science and Education of the Russian Federation in the framework of the Federal Target Program "Scientific and Pedagogical Personnel of Innovative Russia" for 2009–2013 (agreement no. 14.B37.21.0571), as well as by grants nos. MD-97.2013.8 and SP-1051.2012.4 of the President of the Russian Federation.

REFERENCES

1. Paital, S.R. and Dahotre, N.B., Calcium phosphate coatings for bio-implant applications: materials, performance factors, and methodologies, *Mater. Sci. Eng. R.*, 2009, vol. 66, pp. 1–70.
2. Dorozhkin, S.V., Bioceramics of calcium orthophosphates, *Biomaterials*, 2013, vol. 31, pp. 1465–1485.
3. Lapaj, L., Markuszewski, J., Rybak, T., Britsko, A.A., Anosov, V.V., and Wierusz-Kozlowska, M., Wear analysis of a ceramic on ceramic hip endoprostheses, *J. Friction Wear*, 2013, vol. 34 (1), pp. 32–37.
4. Grushko, A.V., Sheykin, S.E., and Rostotskiy, I.Yu., Contact pressure in hip endoprostethic swivel joints, *J. Friction Wear*, 2012, vol. 33 (2), pp. 124–129.
5. Shtansky, D.V., Petrzhik, M.I., Bashkova, I.A., Kiryukhantsev-Korneev, F.V., Sheveiko, A.N., and Levashov, E.A., Adhesion, friction, and deformation characteristics of Ti-(Ca,Zr)-(C,N,O,P) coatings for orthopedic and dental implants, *Phys. Solid State*, 2006, vol. 48, no. 7, pp. 1301–1308.
6. Fomin, A.A., Rodionov, I.V., Steinhauer, A.B., Fomina, M.A., Zakharevich, A.M., Skaptsov, A.A., and Petrova, N.V., Structure of composite biocompatible titania coatings modified with hydroxyapatite nanoparticles, *Adv. Mater. Res.*, 2013, vol. 787, pp. 376–381.
7. Rodionov, I.V., Application of the air-thermal oxidation technology for producing biocompatible oxide coatings on periosteal osteofixation devices from stainless steel, *Inorg. Mater.: Appl. Res.*, 2013, vol. 4, no. 2, pp. 119–126.
8. Fomin, A.A., Shteingauer, A.B., Rodionov, I.V., Petrova, N.V., Zakharevich, A.M., Skaptsov, A.A., and Gribov, A.N., Nanostructure of titanium dioxide coatings modified by hydroxyapatite on medical titanium implants, *Meditsinskaya Tekh.*, 2013, no. 3, pp. 24–27.
9. Solntsev, K.A., Zufman, V.Yu., Alad'ev, N.A., Shevtsov, S.V., Chernyavskii, A.S., and Stetsovskii, A.P., Titanium-to-rutile oxidation kinetics in the direct-oxidation fabrication of thin-wall ceramics, *Inorg. Mater.*, 2008, vol. 44, no. 8, pp. 969–975.
10. Gritsenko, B.P., Ivanov, Yu.F., Koval', N.N., Krukovskii, K.V., Girsova, N.V., Teresov, A.D., Ratochka, I.V., and Mishin, I.P., Regularities of the formation and the role of secondary structures in the improvement of the wear resistance of commercially pure titanium VT1-0, *J. Friction Wear*, 2012, vol. 33, no. 3, pp. 184–189.

Translated by D. Tkachuk